

Self-Supervised Learning for Single-Molecule Localization Microscopy Denoising

Clare Minnerath

Providence College
Providence, RI, USA

cminnera@friars.providence.edu

Jonathan Ventura

California Polytechnic State University
San Luis Obispo, CA, USA
jventu09@calpoly.edu

Guy Hagen

U. of Colorado Colorado Springs
Colorado Springs, CO, USA
ghagen@uccs.edu

Abstract

We evaluate the ability of self-supervised deep learning for Poisson denoising of Single-Molecule Localization Microscopy (SMLM) in addition to the impact denoising can have on the ability to locate molecules within the Single-Molecule Localization Microscopy images. SMLM images are predominantly corrupted with Poisson noise. There are currently existing methods for producing super-resolved SMLM images. However, there is a need for more accurate SMLM images in order for scientists to gain a better understanding of the functions of live cells at the nanoscale. By denoising SMLM images prior to the images undergoing the current state-of-the-art super-resolution techniques, we create a less corrupted version of SMLM images. As a result, the exact locations of the molecules in the images can be determined with more accuracy and precision. We denoise SMLM images utilizing only the original noisy images as training data with a Self-Supervised Deep Learning model. By modifying the previous Self-Supervised techniques that have been successful in denoising images with Gaussian noise, we remove Poisson noise from SMLM images.

Introduction

Since a majority of biological processes occur at the nanoscale, the ability to study cell and molecular behavior at this scale is critical for scientists. Specifically, the knowledge of nanoscale functions can help medical researchers design tools, treatments, and therapies that are more precise and personalized than conventional ones (Nano.gov).

Due to the effects of diffraction, classic optical microscopes are only able to resolve structures larger than 200nm (Allen et al. 2016). Single Molecule Localization Microscopy is a key technology for creating nanoscale images with optical microscopes. Using both super-resolution techniques and statistically locating individual molecule's blinks to sub-pixel resolution, SMLM is able to produce a new image which compiles the individually detected molecules together. The more exact SMLM can be in detecting and locating individual molecule blinks is a determining factor in how concise the location of the molecules can be determined. So, there is still room for improvement in locating individual molecules with more accuracy than is currently possible from noisy SMLM images due to the fact that the

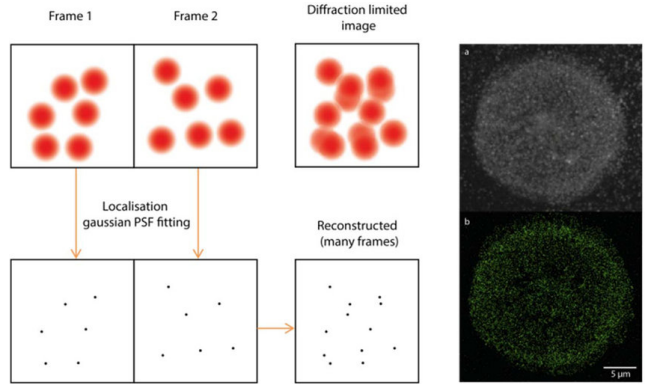


Figure 1: Process of SMLM localization and reconstruction to surpass the diffraction barrier (Shannon et al. 2015).

noise within an image makes pinpointing each molecule's true signal difficult.

SMLM images are taken as light is absorbed by the molecules, and, as a result, the molecules randomly emit light of a larger wavelength in small blinks which are captured by the camera. Because the blinks only emit a small number of photons, the resulting images are very noisy. Due to the dynamic blinking and low light levels in SMLM images, only a single noisy instance of a signal is available for a given instance of an image. Without a clean version of an image's signal, the use of a traditional deep learning approach that trains by mapping noisy images to the corresponding clean ones is not possible.

A current state-of-the-art super-resolution technique which utilizes deep networks is DeepSTORM, a CNN that trains on simulated and experimental data (Nehme et al. 2018). However, this method, although it has strong super-resolution performance, does not use any localization techniques which are vital in SMLM. Therefore, this method is not a practical solution for locating molecules on the nanoscale.

Traditionally, the best performance in deep learning approaches for image restoration and the denoising of corrupted images has been done using a supervised deep network that utilizes pairs of corresponding corrupt and clean images. In particular, there are content-aware image restora-

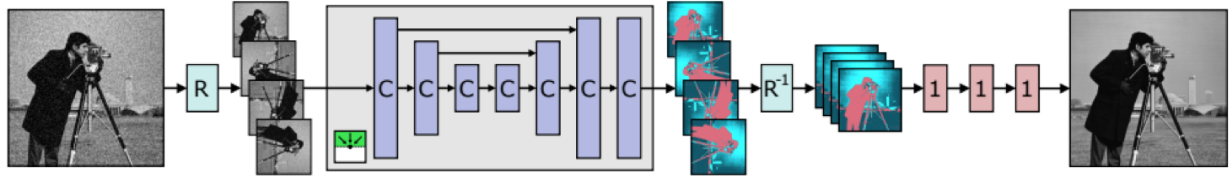


Figure 2: Proposed blind-spot network architecture for denoising SMLM images (Laine et al. 2019)

tion (CARE) networks that have proven useful for denoising fluorescence microscopy data given noisy and clean images (Weigert et al. 2018). Techniques such as these are rendered useless when considering SMLM data which has no way of obtaining clean images.

Related Work

New findings have shown that despite the limitations of solely individual noisy SMLM images, denoising to the performance level of supervised deep networks could be possible. The work of Lehtinen et al. (2018) shows that it is no longer necessary to provide a clean instance of an image. In NOISE2NOISE (N2N), they show by training using pairs of two corresponding noisy images that share the same signal, it is possible to achieve equal quality, if not higher quality (when training with finite data), performance for denoising. This method still requires at least 2 noisy realizations of an image's signal.

Building off the ideas from N2N, NOISE2VOID (N2V) shows that one can build a model for denoising using only individual noisy images for training data (Self-Supervised) (Krull, Buchholz, and Jug 2018). N2V introduces the use of a blind-spot network which masks a pixel's data from the network's receptive field and allows the data surrounding the said blind-spot to effectively predict the the pixel's signal. The N2V model is limited because it assumes every pixel's signal is dependent of the signals surrounding it.

To address the limitation of N2V, Laine et al. (2019) designed a different blind-spot architecture that uses 4 different receptive fields to allow every pixel in the image to contribute to the loss function while maintaining the blind-spot. This differs from N2V which selected a smaller receptive field from within the image. In order to predict the blind-spot pixel's signal, they apply a maximum a posteriori estimation (MAP) denoising procedure during testing that allows for the prediction of the clean signal to take into account the masked pixel. This method can perform on par with the supervised traditional deep denoising models under the assumption of Gaussian noise in the data.

Laine et al. does include a model for Poisson noise. But, in a manner impractical to SMLM images, their model uses a Gaussian approximation to represent the Poisson noise distribution. This method is impractical because the signal from SMLM is low, which causes a Gaussian approximation does not accurately represent the Poisson noise present in SMLM images.

More continued work since N2V also attempts to pre-

dict the blind-spot pixel without the assumption of a Gaussian noise model (Krull, Vicar, and Jub 2019). The PROBABILISTICNOISE2VOID (PN2V) model trains a probability distribution for 800 possible output values for a given pixel. PN2V is able to out perform N2V using the same U-Net architecture, but does not perform to the level of traditional supervised techniques. PN2V is working with discrete values for its pixel distribution which makes it a good fit to combat Poisson noise efficiently. But, since SMLM images are 16-bit, each pixel has 2^{16} possible values. Since SMLM images have such a large possible range in pixel values and the PN2V method shows success using a distribution of 800 possible output values, PN2V is not the optimally suited for denoising SMLM.

Research Questions

1. How well can self-supervised learning denoise SMLM images?

Hypothesis: By modifying the work which successfully denoises images with Gaussian noise, it will be possible to denoise SMLM images to the levels of other self-supervised denoising models.

2. Does denoising SMLM images prior to localization techniques and super-resolution improve the ability to locate molecule positions compared to just using current localization and super-resolution techniques on noisy images?

Hypothesis: Given SMLM currently depends on the noisy signals from the blinking molecules, by denoising the images prior to detecting and locating the molecules, our localizing abilities will be more precise. This is because the signal from the blinking molecules will be more representative of the molecules exact position in an image that is not corrupted with noise.

Method

By utilizing the blind-spot architecture designed by Laine et al. (Figure 2), which rotationally obscures the middle pixel, while also implementing an adjusted method for training the model and predicting the blind-spot signal's output, we are able to remove Poisson noise from SMLM images. In the process described by Laine et al. (2019), Poisson noise is approximated by considering a Gaussian distribution with $\sigma^2 = \lambda$. This estimate will only provide a strong approximation when the standard deviation within the Poisson noise is small and the image's signal is large.

To better train our network and more accurately estimate a masked pixel's signal while considering the Poisson noise present in SMLM, we created a process that can model the Poisson noise while producing non-discrete clean signal values. Using the Poisson probability mass function (Equation 1), it is possible to represent a distribution for the Poisson noise present in SMLM images.

$$P(Z = z) = \frac{\lambda^z \exp(-\lambda)}{z!} \quad (1)$$

We minimized the likelihood of the noisy pixel values over all possible clean values (Equation 2) to train our self-supervised denoising model.

$$P(Z_i = z_i) = \int_0^\infty P(Z_i = z_i | X_i = x) P(X_i = x) dx \quad (2)$$

Since we only have the noisy image signals, Z_i , our loss function must be representative of these known values. To do this we introduced the conjugate prior for the Poisson Distribution, the Gamma distribution. By representing the distribution of possible clean image signals, X_i , by the Gamma distribution, it is possible to marginalize out the clean realization of our image which is unknown in SMLM (Equation 3).

$$\begin{aligned} P(Z_i = z_i) &= \int_0^\infty \frac{\beta^\alpha}{\Gamma(\alpha)} \cdot \frac{x^{z_i + \alpha - 1} e^{-(x - \beta x)}}{z_i!} \\ &= \frac{\beta^\alpha}{(1 + \beta)^{\alpha + z_i}} \cdot \frac{\Gamma(\alpha + z_i)}{\Gamma(\alpha)} \cdot \frac{1}{z_i!} \end{aligned} \quad (3)$$

Using this marginalized equation, the negative log likelihood loss function can be calculated without using an approximation (Equation 4).

$$\begin{aligned} \mathcal{L}_i &= -\log \left(\frac{\beta^\alpha}{(1 + \beta)^{\alpha + z_i}} \cdot \frac{\Gamma(\alpha + z_i)}{\Gamma(\alpha)} \cdot \frac{1}{z_i!} \right) \\ &= -\alpha \log(\beta) + (\alpha + z_i) \log(1 + \beta) \\ &\quad - \log(\Gamma(\alpha + z_i)) + \log(\Gamma(\alpha)) + \log(\Gamma(z_i + 1)) \end{aligned} \quad (4)$$

In order for the obscured pixel value to contribute to the clean pixel estimation, the best results were obtained using the Gamma posterior mean (Equation 5). This preformed better than the a the Gamma MAP estimation which tended to weigh the noisy pixel value too heavily.

$$\text{Gamma Posterior Mean: } x_i = \frac{\alpha + z_i}{\beta + 1} \quad (5)$$

For each YFP dataset we trained a separate model. Because of differences in noise levels and molecule shapes, the best results for denoising were produced by training and validating on 1000 images cropped to 512x512 pixels from a

single dataset. Best results were obtained when the model is trained on images with a average to slightly higher signal. So images with little to no signal comparatively to the rest of the dataset were not included in the training batch. After training the networks using single 900 image batches with 100 validation images, the networks could then successfully denoise the entirety of the respective datasets. Training the model for each individual dataset is feasible because it takes between 12-18 epochs to train at approximately 6 minutes per epoch.

The visibly denoised images are then processed using the ImageJ Plugin, ThunderSTORM (Ovesn et al. 2014; Schneider, Rasband, and Eliceiri 2012). We then compared the results from the processed denoised images to the processed noisy images. We used this comparison as well as the results from testing on simulated datasets to make sure our model is removing the noise while retaining the true signal from SMLM images.

Evaluation

Data

To train and test our model we used two single molecule microscopy datasets of yellow fluorescent protein (YFP)-tagged growth factor receptors taken from human Epithelial carcinoma A431 cells expressing mCitrine-ErbB3 (Luke et al. 2018). Since this dataset uses YFP-tagged receptors rather than traditional dye, the molecules emit less photons than most SMLM images. As a result, the YFP datasets have low signal to noise ratio making them good candidates for denoising.

We also evaluated our model using simulated datasets. Simulated data will be useful for testing the accuracy of the localizing from our denoised data. Testing this allows us to gain some verification that the model does not alter the true signal or add signal from non-existing molecules because ground truth molecule locations are known for this data set. Using the ThunderSTORM Performance Testing tool we created 7 simulated data sets. One of the created data sets used the default simulation setting and was tested on all models. For the other 6 datasets, we created two groups each with 3 simulated datasets. Each group of data imitates one of two real YFP data sets at 3 different levels of noise resulting 6 more generated datasets.

Metrics

To evaluate how well our model is able to denoise the SMLM images we looked at the signal to background ratio (SBR). In order to find the SBR, there needed to be a way of distinguishing the background from the foreground. By implementing an automatic iterative threshold selection commonly used for gray-scale image thresholding, it was possible to determine a signal threshold to separate the signal from the background (Svoboda, Kybic, and Hlavac 2007). We hoped this metric would give a marker of how well our model is denoising given we have no clean image comparison to compare our results to. However, even when the results qualitatively appeared to improve and the localization uncertainty lowered, the SBR of a resulting image was not

necessarily greater than its noisy pair. Using the signal to background ratio is also not an ideal way to generally assess denoising because our model could successfully denoise the black background without having the same effect across the entirety of the image. For these reasons, we solely look at the qualitative results from the denoising model prior to utilizing our super-resolution and localization techniques. Then, if there is improvement in the ability to locate molecules in comparison to the localization ability on the images without denoising, it can be assumed that the denoising our model achieved occurred across the entirety of the image.

Once we have qualitatively determined our model's ability to denoise the SMLM images, we then evaluated the effect the denoising model had on the ability to locate individual molecules within the images. For this we used ThunderSTORM. ThunderSTORM is a SMLM image processing, analyzing, and visualizing tool (Ovesn et al. 2014). ThunderSTORM can be implemented as a plugin for the image processing application ImageJ (Schneider, Rasband, and Eliceiri 2012). It is particularly helpful in assessing a threshold for detection of molecules in raw and filtered images. So, in order to evaluate a potential improvement in the denoised images threshold for detection, we will first run the raw/noisy YFP data through ThunderSTORM and record the results. Then, we will denoise the YFP data with our Self-supervised denoising model. Finally, we will run the denoised data through ThunderSTORM once more and compare the threshold for detection results between the raw and denoised data. Along with this quantitative data, Thunder-

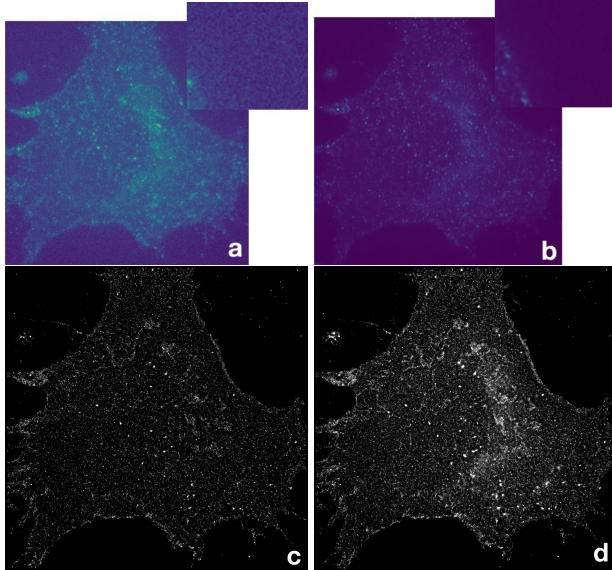


Figure 3: YFP-Dataset 3 denoising visual results: (a) Single noisy YFP image with an additional zoom of the top right corner. (b) Single corresponding denoised YFP image with an additional zoom of the top right corner. (c) Image compiled from molecule localization from all YFP-dataset 3 noisy images. (d) Image compiled from molecule localization from all denoised YFP-dataset 3 images.

STORM has a visualization tool that creates a new image of the cell by compiling the detected molecules locations together. So, a final visual result can also be compared between the noisy and denoised datasets.

Results

After training and testing using the self-supervised denoising model on yellow fluorescent protein (YFP)-tagged data, there have been improvements in both the reduction of noise in the image (evaluated qualitatively) and the ability to locate individual molecules within the SMLM images.

Despite the Signal to Background Ratio metric not being a quality measure of the noise in the images, it is not difficult to qualitatively evaluate the denoising process. In Figures 3 and 4, images (a) and (b) from YFP-dataset 3 as well as images (e) and (f) from YFP-dataset 4 demonstrate the models ability to pick out the signal amongst noise. Images (b) and (f) do not appear to have as much signal as their noisy counterparts images (a) and (e). But, the difference is due to the noise being amplified in areas of signal in images (a) and (e), not a loss of molecule signal. The ability to get rid of the excess noise around the signal allows for individual molecules to be pinpointed. In an area where multiple molecules are close together, their respective noise can blur together making it unfeasible to locate each molecule individually with

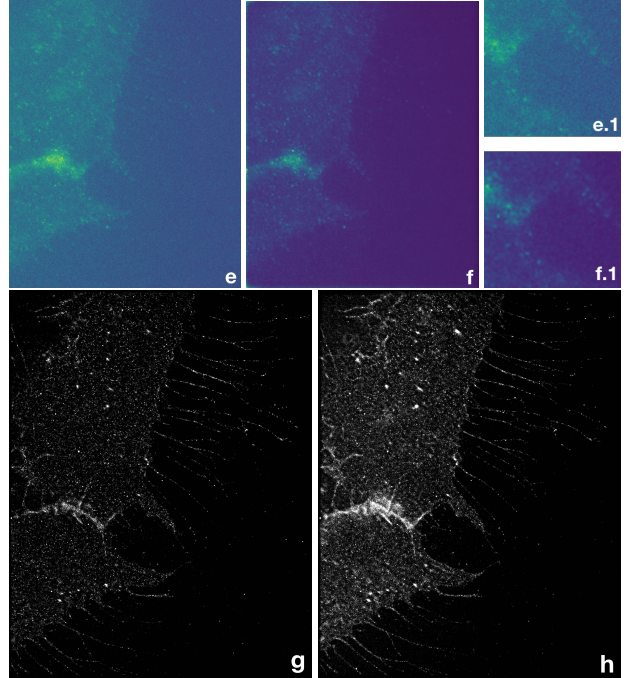


Figure 4: YFP-Dataset 4 denoising visual results: (e) Single noisy YFP image. (e.1) An additional zoom from image (e). (f) Single corresponding denoised YFP image. (f.1) An additional zoom from image (f). (g) Image compiled from molecule localization from all YFP-dataset 4 noisy images. (d) Image compiled from molecule localization from all denoised YFP-dataset 4 images.

Data	Molecules Located	Mean Sigma [nm]	Standard Dev. Sigma [nm]	Mean Uncertainty [nm]	Standard Dev. Uncertainty [nm]
Noisy YFP-Dataset 3	364,509	104.8981	62.35194	17.43365	5.770702
Denoised YFP-Dataset 3	882,188	111.466	60.64917	13.46961	6.124521
Noisy YFP-Dataset 4	153,061	109.2096288	88.81489875	17.08962255	6.198097691
Denoised YFP-Dataset 4	974,163	138.215115	101.79013	16.9050282	5.87430829

Table 1: Molecule localization data obtained using ThunderSTORM with default settings + EM Gain = 150.0 for YFP-Dataset 3 and EM Gain 100.0 for YFP-Dataset 4. Post-processing with ThunderSTORM: Duplicate removal and drift correction.

Data	True Positives	False Positives	False Negatives	Jaccard Index	Precision	Recall	F1
Noisy Simulated	150,630	3,790	16,874	0.879	0.975	0.899	0.936
YFP-3 Model	156,795	3,899	10,709	0.915	0.976	0.936	0.955
YFP-4 Model	156,136	4,178	11,341	0.91	0.974	0.932	0.953

Table 2: Performance evaluation results from the ThunderSTORM simulated dataset using the default settings. The data from each row is the result of a comparison between the dataset’s localizations and the ground truth molecule locations.

any certainty. To locate each molecule in an SMLM image, ThunderSTORM fits a Gaussian distribution to the signals from the image. Using the data from the Gaussians at each

point, it can be determined whether a molecule is present, where it is present, and a location uncertainty value. We know more molecules can be located in the denoised images because of the compiled images produced as well as the localization data found in Table 1.

Table 1 shows the results of the analysis of the original noisy image sets in comparison with analysis of the denoised image sets. Sigma is the standard deviation of the gaussian fit to a molecules signal and the uncertainty measure is calculated using a combination of this value, the intensity of the signal, and other parameters from the gaussian distribution. Using ThunderSTORM it was possible to locate more than double the amount of molecules with the denoised data compared to the original corrupted data. Both models were able to make these large jumps in localizaion of molecules while still maintaining lower mean uncertainties.

Applying our denoising networks to simulated data also produced improvements in visual denoising and molecule locating. Using the ground truth molecule locations it is possible to determine how many molecules are being accurately located as well has the number of false positive and false negative molecule localizations. For our experiments, a localization of a molecule is considered correct if it is within 50nm of the ground truth location (default setting). The results from our simulated data give reassurance in our de-noised molecule localization numbers from the real data.

Utilizing the ThunderSTORM simulated data default noise and signal settings, we created a 1,000 image dataset. Table 2 and the bottom images in Figure 5 display the results of the models which were trained on real data being used to denoise the ThunderSTORM default simulated dataset. The left of the bottom right two images is the output of the model trained on YFP-dataset 3 and the right of the two is the output of the model trained on YFP-dataset 4. Both models produced images which were able to detect more true molecule locations than the original noisy image set. However, on this specific dataset both model’s output images had more false positive localizations than from the noisy data. We speculate that a model trained and tested on data with different levels

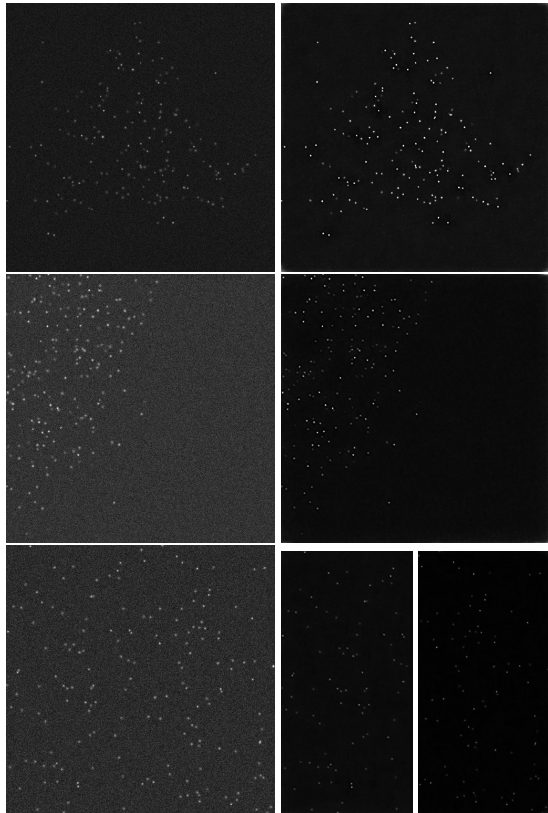


Figure 5: Single noisy ThunderSTORM simulated images on the left with the corresponding denoised images on the right. From top to bottom: generated data simulating YFP-dataset 3 (Mean Noise Level = 150.0 photons), generated data simulating YFP-dataset 4 (Mean Noise Level = 150.0 photons), generated data using default settings.

Noise Level	Data	True Positives	False Positives	False Negatives	Jaccard Index	Precision	Recall	F1
50.0	Noisy	167,163	7,075	14,690	0.885	0.959	0.919	0.939
	Denoised	171,418	2,847	10,435	0.928	0.984	0.943	0.963
100.0	Noisy	166,354	7,768	15,253	0.878	0.955	0.916	0.935
	Denoised	169,642	3,979	11,965	0.914	0.977	0.934	0.955
150.0	Noisy	165,023	8,466	16,258	0.870	0.951	0.910	0.930
	Denoised	167,947	5,890	13,334	0.897	0.966	0.926	0.946

Noise Level	Data	True Positives	False Positives	False Negatives	Jaccard Index	Precision	Recall	F1
50.0	Noisy	167,814	11,855	24,052	0.824	0.934	0.875	0.903
	Denoised	169,974	6,407	21,892	0.857	0.964	0.886	0.923
100.0	Noisy	165,988	12,903	25,867	0.811	0.928	0.865	0.895
	Denoised	167,174	8,514	24,681	0.834	0.952	0.871	0.910
150.0	Noisy	163,058	13,732	28,328	0.795	0.922	0.852	0.886
	Denoised	163,228	12,032	28,158	0.802	0.931	0.853	0.890

Table 3: Performance evaluation results from ThunderSTORM generated data imitating YFP-dataset 3 (above) and YFP-dataset 4 (below) at three different mean background noise levels (photons). The data from each row is the result of a comparison between the dataset’s localizations and the ground truth molecule locations.

of signal and noise leads to lower quality denoising performance and therefore lower localization abilities. Nonetheless, the overall result is that all the similarity indexes are improved by the model’s denoised images except the precision of localization in the images from the YFP-4 model.

To better represent the real data that our models were trained on, we generated simulated data with a comparable signal intensity range as well as comparable full width at half maximum range for the molecule signal spread to the real YFP datasets. Using a mask (thresholded image) from the original YFP-dataset, the ThunderSTORM data generator spreads the signal intensities according to the mask’s values. We then replicated the simulation at 3 different noise levels for both of the datasets since the level of noise throughout the real YFP images frames is not uniform. Each dataset consisted of 1,000 images and was tested on the network trained on the data it is simulating. After processing the noisy data and model’s output, the produced molecule localizations are compared with the ground truth locations. As can be seen in Table 3, at each level of noise both of the model’s are able to pinpoint more molecules while maintaining less false positives and false negatives than the noisy data. As a result, the similarity indexes are higher at every point for the denoised data in comparison with the original simulated noisy data. An example of the qualitative denoising results from the model on the simulated data can be seen in Figure 5. So, our models, when trained at certain signal intensities/noise levels, are able to produce denoised images which accurately locate higher numbers of molecules in a given dataset.

Conclusion

We have developed and evaluated a self-supervised deep learning model for denoising Single Molecule Localization Microscopy images which are corrupted with Poisson noise.

To do this, we built off recent research in self-supervised denoising models and fit the techniques to denoise images taken in low light conditions (images containing large amounts of Poisson noise). As a result of the denoising, there has been no correlation with the Signal to Background metric. However, utilizing the ImageJ plugin, ThunderSTORM, we have been able to see an improvement in detecting and locating individual molecules within SMLM images. Reproducing positive results on real data as well simulated data has shown that our models are able denoise SMLM images without distorting the true image signal. By locating more molecules and continuing farther past diffraction barrier, we hope to create better SMLM images which will allow biologists to advance the studies of cell and molecular behavior at the nanoscale.

Acknowledgement

The work reported in this paper is supported by the National Science Foundation under Grant No. 1659788. Any opinions, findings and conclusions or recommendations expressed in this work are those of the author(s) and do not necessarily reflect the views of the National Science Foundation.

References

- Allen, J.; Silfies, J.; Schwartz, S.; and Davidson, M. 2016. Single-molecule super-resolution imaging. *Nikons MicroscopyU*.
- Krull, A.; Buchholz, T.-O.; and Jug, F. 2018. Noise2void-learning denoising from single noisy images. *arXiv preprint arXiv:1811.10980*.
- Krull, A.; Vicar, T.; and Jub, F. 2019. Probabilistic noise2void: Unsupervised content-aware denoising. *arXiv preprint arXiv:1906.00651*.

Laine, S.; Karras, T.; Lehtinen, J.; and Aila, T. 2019. High-quality self-supervised deep image denoising. *arXiv preprint arXiv:1901.10277*.

Lehtinen, J.; Munkberg, J.; Hasselgren, J.; Laine, S.; Karras, T.; Aittala, M.; and Aila, T. 2018. Noise2noise: Learning image restoration without clean data. *arXiv preprint arXiv:1803.04189*.

Luke, T.; Pospil, J.; Fliegel, K.; Lasser, T.; and Hagen, G. 2018. Supporting data for quantitative super-resolution single molecule microscopy dataset of yfp-tagged growth factor receptors. *GigaScience Database*.

What's so special about the nanoscale? *Official website of the United States National Nanotechnology Initiative*.

Nehme, E.; Weiss, L. E.; Michaeli, T.; and Shechtman, Y. 2018. Deep-storm: super-resolution single-molecule microscopy by deep learning. *Optica* 5(4):458–464.

Ovesn, M.; Kek, P.; Borkovec, J.; vindrych, Z.; and Hagen, G. M. 2014. Thunderstorm: a comprehensive imagej plug-in for palm and storm data analysis and super-resolution imaging. *Bioinformatics* 30(16):23892390.

Schneider, C. A.; Rasband, W. S.; and Eliceiri, K. W. 2012. Nih image to imagej: 25 years of image analysis. *Nature Methods* 9:671675.

Shannon, M.; Burn, G.; Cope, A.; Cornish, G.; and M Owen, D. 2015. Protein clustering and spatial organization in t-cells. *Biochemical Society transactions* 43:315–21.

Svoboda, T.; Kybic, J.; and Hlavac, V. 2007. *Image Processing, Analysis & and Machine Vision - A MATLAB Companion*. Thomson Learning, 1st edition.

Weigert, M.; Schmidt, U.; Boothe, T.; Mller, A.; Dibrov, A.; Jain, A.; Wilhelm, B.; Schmidt, D.; Broaddus, C.; Culley, S.; Rocha-Martins, M.; Segovia-Miranda, F.; Norden, C.; Henriques, R.; Zerial, M.; Solimena, M.; Rink, J.; Tomancak, P.; Royer, L.; Jug, F.; and Myers, E. W. 2018. Content-aware image restoration: pushing the limits of fluorescence microscopy. *Nature Methods*.